

Supplementary Material

Climate change and the increasing impact of polar bears on bird populations

Jouke Prop, Jon Aars, Bård Jørgen Bårdsen, Sveinn Are Hanssen, Claus Bech, Sophie Bourgeon, Jimmy de Fouw, Geir Wing Gabrielsen, Johannes Lang, Elin Noreen, Thomas Oudman, Benoit Sittler, Lech Stempniewicz, Ingunn Tombre, Eva Wolters and Børge Moe

[Supplement 1](#). Additional information on methods and study areas.

[Supplement 2](#). Graphs depicting ice concentrations by date and year for each of the sample areas.

[Supplement 3](#). Statistical trends in ice measures over the years for each sample area.

[Supplement 4](#). Results of statistical modelling.

Supplement 1. Information on methods and study areas

Methods – Study areas

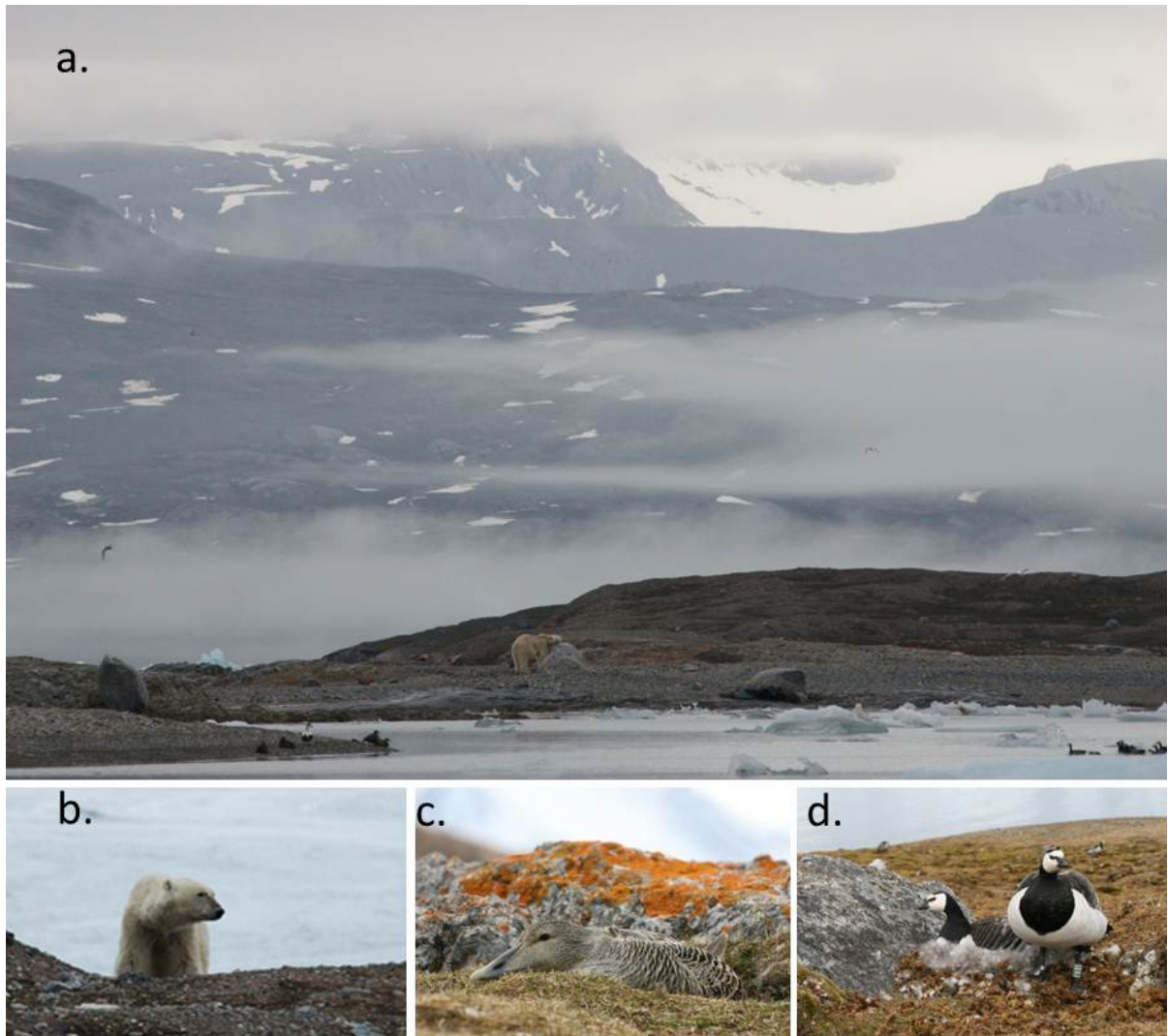


Suppl. 1-Figure S1. Study locations on Spitsbergen (Svalbard, location 1–4) and in Greenland (location 5): 1= Hornsund, 2= Bellsund, 3= Nordenskiöldkysten, 4= Kongsfjorden and 5= Traill Island. Red hatched areas denote the scale of the areas covered by observations. a: Colonies of ground-breeding birds, b: bird cliffs, c: tundra areas with breeding birds.

In Hornsund (1) observations were done by biologists in the area around the Polish Polar Station delineated by Hansbreen and Revelva, located 2 and 3 km to the east and west, respectively. In Bellsund (2) observations were done on Eholmen. This island is 0.5 km² and hosts breeding common eiders, barnacle geese and glaucous gulls. The island is managed as an eider farm with down harvesting and observations were done by a trapper and his assistants. On Nordenskiöldkysten (3) observations were done by biologists based in a camp at Vinkelvatnet, close to Diabasøya, covering an area of up to 10 km from the camp. In Kongsfjorden (4) observations were done by biologists based in Ny-Ålesund and working in the bird colonies on the islands and in the bird cliffs. Hence, observations covered the inner 10 km of the fjord. On Traill Island observations were done by biologists based at Holm Bugt hut in Karupelv Valley, covering an area of approximately 5 km from the base.

Suppl. 1-Table S1. Number of days with observers present at the different locations.

Year	1 June–31 July				15 June–15 Aug
	Hornsund	Bellsund	Nordenskiöldkysten	Kongsfjorden	Traill Island
1972	47	-	-	-	-
1973	47	-	-	-	-
1974	45	-	-	-	-
1975	38	-	-	-	-
1976	-	-	-	-	-
1977	40	-	56	-	-
1978	-	-	61	-	-
1979	45	-	51	-	-
1980	45	-	61	-	-
1981	46	-	61	-	-
1982	46	-	-	28	-
1983	38	-	-	-	-
1984	38	-	10	-	-
1985	38	-	-	-	-
1986	38	-	22	28	-
1987	-	50	-	-	-
1988	40	50	20	-	45
1989	-	25	61	-	38
1990	-	25	-	28	41
1991	-	50	16	-	45
1992	-	25	-	47	56
1993	54	25	15	42	61
1994	-	50	-	42	41
1995	54	50	14	42	50
1996	54	50	-	44	52
1997	-	50	16	61	53
1998	54	50	-	54	61
1999	-	50	17	51	61
2000	54	50	28	50	61
2001	54	50	-	51	51
2002	-	50	-	45	51
2003	54	50	21	46	41
2004	54	50	60	45	46
2005	38	25	-	45	61
2006	44	50	-	51	49
2007	44	50	22	56	42
2008	44	50	31	61	42
2009	44	50	37	56	40
2010	44	25	52	46	32
2011	44	-	53	34	42
2012	44	-	54	46	42
2013	-	-	61	45	33
2014	-	-	50	46	-

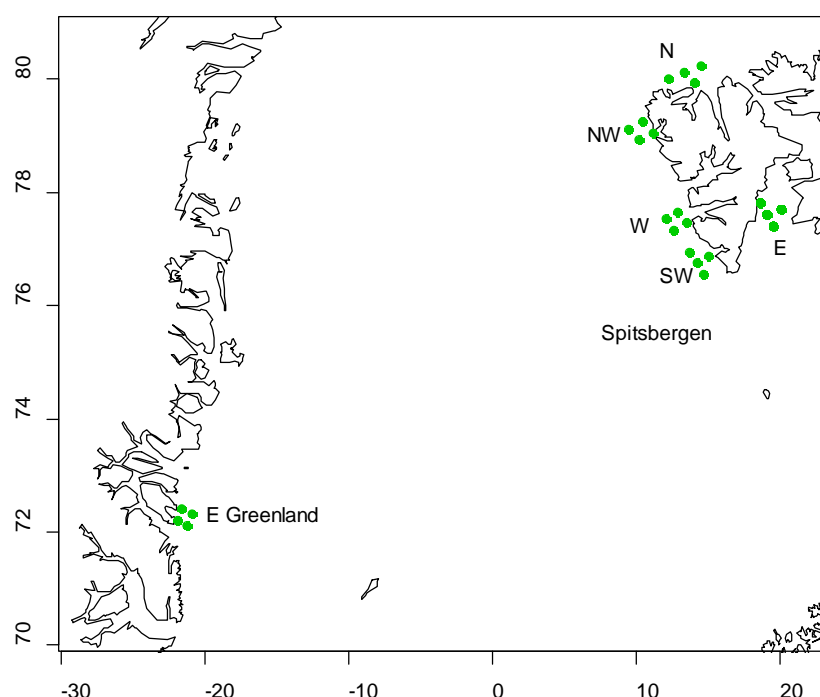


Suppl. 1-Figure S2. The landscape at West Spitsbergen is characterized by fjords, mountains, tundra and glaciers, in addition to the fact that it contains several small islands where colonial birds nest. Pictures of a polar bear is visiting an islet in Kongsfjorden (a, b), and feeding on bird eggs, mainly from common eiders (c) and barnacle geese (d). In this study, long-term time series of polar bear summer sightings have been obtained in four different areas at the coast of west Spitsbergen and one at east Greenland. Photo credit: Børge Moe

Methods – Establishing predation rates, Nordenskiöldkysten

To assess the total number of nests in the study colony without causing disturbance to incubating birds, the island was visited after the geese had left the colony. Nests that had been used in that particular season were identified by the presence of droppings, down, or fresh moss or seaweed. These features were also used to determine which species had used the nest. All used nests (totalling at N_{marked_s}) were marked by numbered stakes. By comparing the marked nests on the island with the marked nests on photographs (monitored from an observation tower throughout incubation) enabled us to determine the proportion of nests that was still recognizable at the time of sampling ($PN_{recovered_s}$). For barnacle goose, this proportion varied among years at 75–85%. The larger nests of glaucous gulls were recovered in all cases. The total number of nests per species was estimated as $N_{total_s} = N_{marked_s} / PN_{recovered_s}$. As the number of eider nests visible from the observation tower was low (many nests were hidden between or behind rocks), we used the estimate of $PN_{recovered}$ obtained from barnacle goose. Some nests were used by several, successive pairs. The average number of nest attempts per nest was $AN_s = N_{attempts_s} / N_{monitored_s}$, with $N_{monitored_s}$ being the number of nests monitored of species s and $N_{attempts_s}$ the number of breeding attempts in these nests. The number of predated goose and gull pairs was estimated as $P_s = PNP_s \times N_{total_s} \times AN_s$, where PNP_s is the proportion of nest attempts predated based on the monitored nests of species s . The number of predated eider nests was estimated from the total number of nests predated by polar bears minus the number of predated nests of geese and gulls: $P_{eider} = P_{bear} - P_{goose} - P_{gull}$. The total number of nests predated by polar bear (P_{bear}) was derived from continuous records of polar bears when present in the colony. For periods that the bears were on the seaward slope of the island, invisible to the observers, the number of nests predated was estimated as the time invisible divided by the average time needed to find and consume the contents of a nest at that particular day. The predation ratio of each of the three species was calculated as $P_{species} / N_{total_{species}}$.

Methods – Large-scale sea ice data



Suppl. 1-Figure S3.

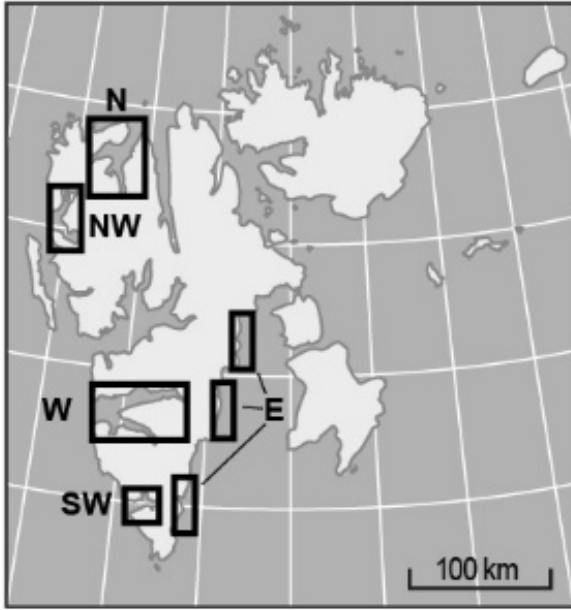
Large-scale data on sea ice concentrations (%) were extracted from six areas: southwest Spitsbergen, west Spitsbergen, northwest Spitsbergen, north Spitsbergen, east Spitsbergen, and east Greenland. For each of the areas ice concentration was extracted from 4 adjacent blocks of 25×25 km (indicated by green dots).

Data on sea ice concentrations were downloaded from the University of Colorado at ftp://sidacs.colorado.edu/pub/DATASETS/nsidc0051_gsfc_nasateam_seaice/final-gsfc/north/daily/. We then extracted daily sea ice concentrations from the period 1979–2013 from six areas composed of four 25×25 km blocks (Fig. S3). The six areas represented large-scale sea ice conditions for polar bears observed in the study locations (Table S2). ICE area 1 refers to the nearest areas. For Spitsbergen, sea ice cover is more extensive in the east and north and polar bear densities are much higher in these areas compared to the western part. Since polar bears may operate on a large spatial scale, we aimed to test whether polar bear incursions on land along the western coast were driven by sea ice conditions in the east and north, and not only at the western coast. Hence, for Spitsbergen, ICE area 2 refers to sea ice extracted from the east and the north. This approach was not required for East Greenland, where ice is more abundant than along the west coast of Spitsbergen; sea ice conditions further north or south would correlate very strongly to the nearest selected area. Sea ice formation and disappearance follows a seasonal pattern with maximum concentrations in late winter (usually March) and minimum in autumn (usually September). We therefore structured each year of data as the period from 1 Sept to 31 Aug (Supplement 2: Figures S1–S6). By using a sea ice concentration of 30% we then calculated two sea ice indices. The **length of the ice season** was calculated as the number of days from the first day with sea ice >30% to the last day with sea ice >30%. The latter was also used to define the **start of the icefree season**. In cases where sea ice concentrations were never above 30% during an ice-year, start of the icefree season was assigned with 0 (1st Jan). We also calculated **monthly mean sea ice concentrations** for April, May, June and July.

Suppl. 1-Table S2. Locations and areas where large-scale ice data were extracted (See Figure S3 for geographic positions of the areas).

Location	ICE area 1	ICE area 2
Hornsund	SW Spitsbergen	E Spitsbergen
Bellsund	W Spitsbergen	E Spitsbergen
Nordenskiöldkysten	W Spitsbergen	E Spitsbergen
Kongsfjorden	NW Spitsbergen	N Spitsbergen
Traill Island	E Greenland	E Greenland

Methods – Fine-scale sea ice data



Suppl. 1-Figure S4. Fine-scale sea ice data were extracted for 2007–2014. The areas were: east Greenland (fjords around Traill Island, not on the map), east Spitsbergen (E), southwest Spitsbergen (SW), west Spitsbergen (W), northwest Spitsbergen (NW) and north Spitsbergen (N). For these coastal areas, ice cover (>70% ice) was estimated.

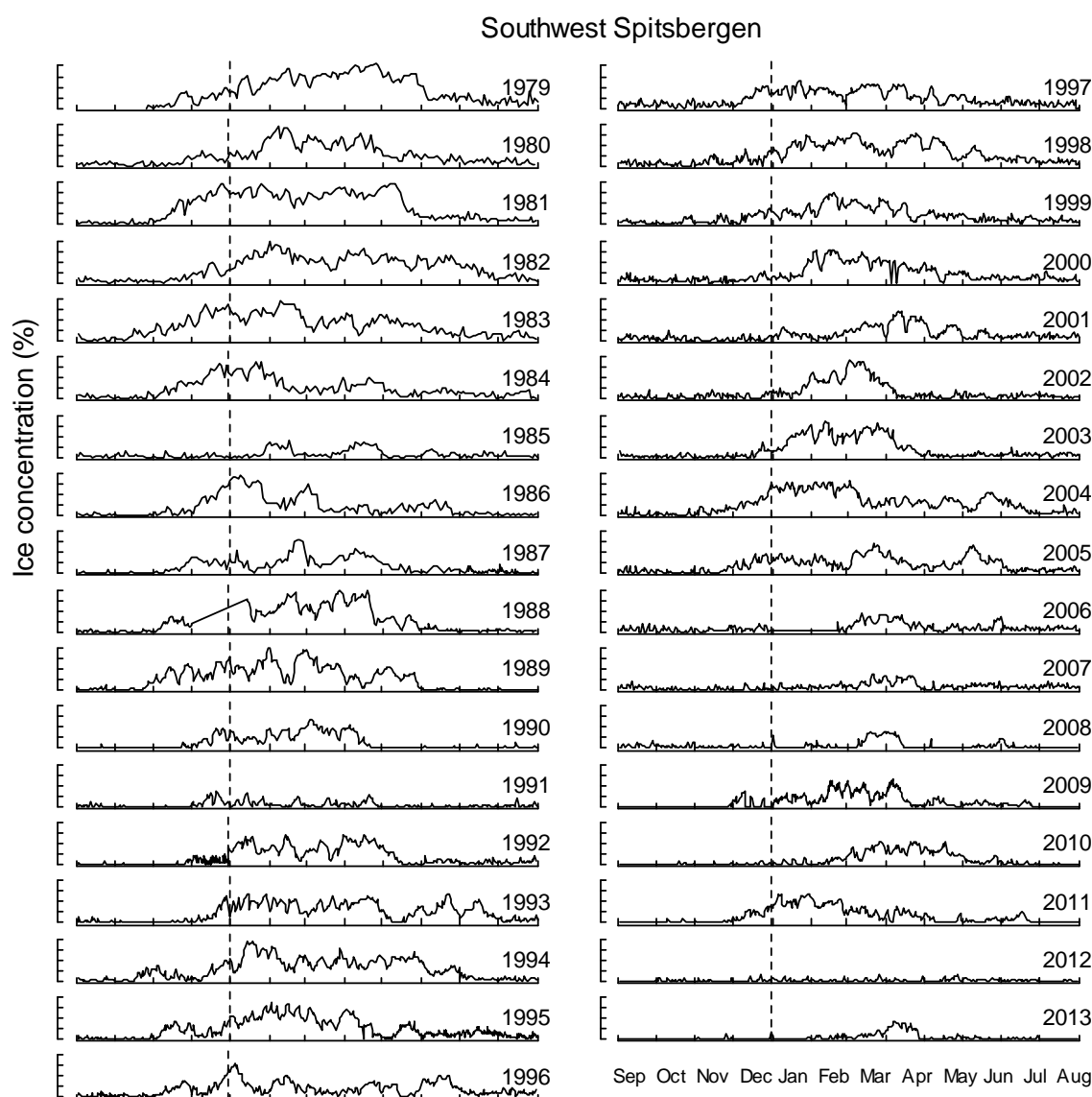
Fine-scale data on sea ice conditions were only available for the most recent years. We downloaded ice maps for 2007–2014 (April–July) from www.met.no/Hav_og_is. These are high-resolution sea ice concentration charts that are mainly based on weather-independent images from the Radarsat-2 satellite. The spatial resolution is sufficiently high (approximately 50 m) to analyse ice conditions in coastal areas, including fjords. Ice concentrations are classified by six categories. For the purpose of our study we selected the three densest categories, i.e. dense drift ice (70%–90% cover), very dense drift ice (90%–100%), and fast ice. Ice data were analysed for the coastal areas of Hornsund (southwest Spitsbergen), Bellsund/Van Mijenfjorden (west Spitsbergen), Kongsfjorden/Krossfjorden (northwest Spitsbergen), Woodfjorden (north Spitsbergen), Isbukta, Kvalvågen, Dunérbukta, and Sørporten (east Spitsbergen), Traill Island (east Greenland) (see Supplement 1, Figure S4). As the scale varied among images, the downloaded maps were first trimmed to obtain images covering a standard geographic area (i.e. the islands of Svalbard, the east coast of Greenland). Using the ImageMagick environment (www.imagemagick.org), the colour range in the images was reduced to correspond to the exact colours of ice density categories, open water and land. Subsequently, the selected coastal locations were identified in the images, and the numbers of pixels for each category were determined and stored for further analysis. For each location and all images from April–July the proportion of area covered by dense ice (*Ice*) was calculated as

$$Ice = (\sum_{i=1}^3 pixel_i) / (\sum_{j=1}^n pixel_j),$$

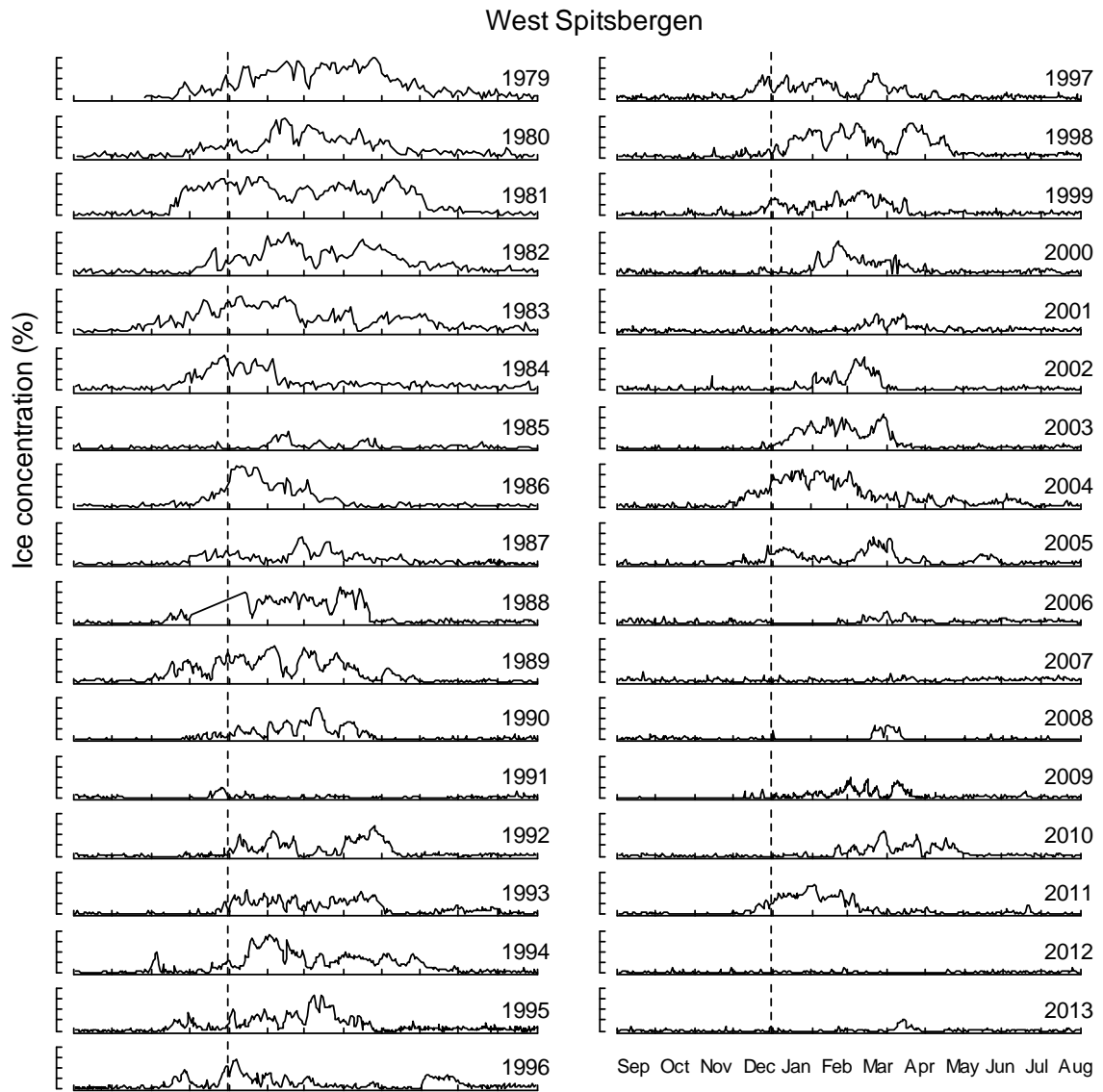
where *pixel* is the number of pixels for a particular category, *i* stands for the three ice categories of interest, *j* stands for all *n* ice concentrations and open water.

Annual ice availability was characterised in two ways. (1) To estimate the average amount of ice, the ice data were aggregated by month (April–July) and subsequently by season. This two-step approach was needed to cope with varying sample sizes due to dates without ice information. (2) Furthermore, the sea ice data were subjected to a non-linear (4-parameter) logistic regression. As a measure of date of peak ice melt we took the inflection point of the curve, which reflects the date of fastest ice disappearance. Estimates with large SE's (exceeding the estimate), which occurred when ice cover was determined by movements of drift ice rather than by melt, were disregarded. In addition, the ice data were aggregated by 5-day periods to describe location-specific melt patterns.

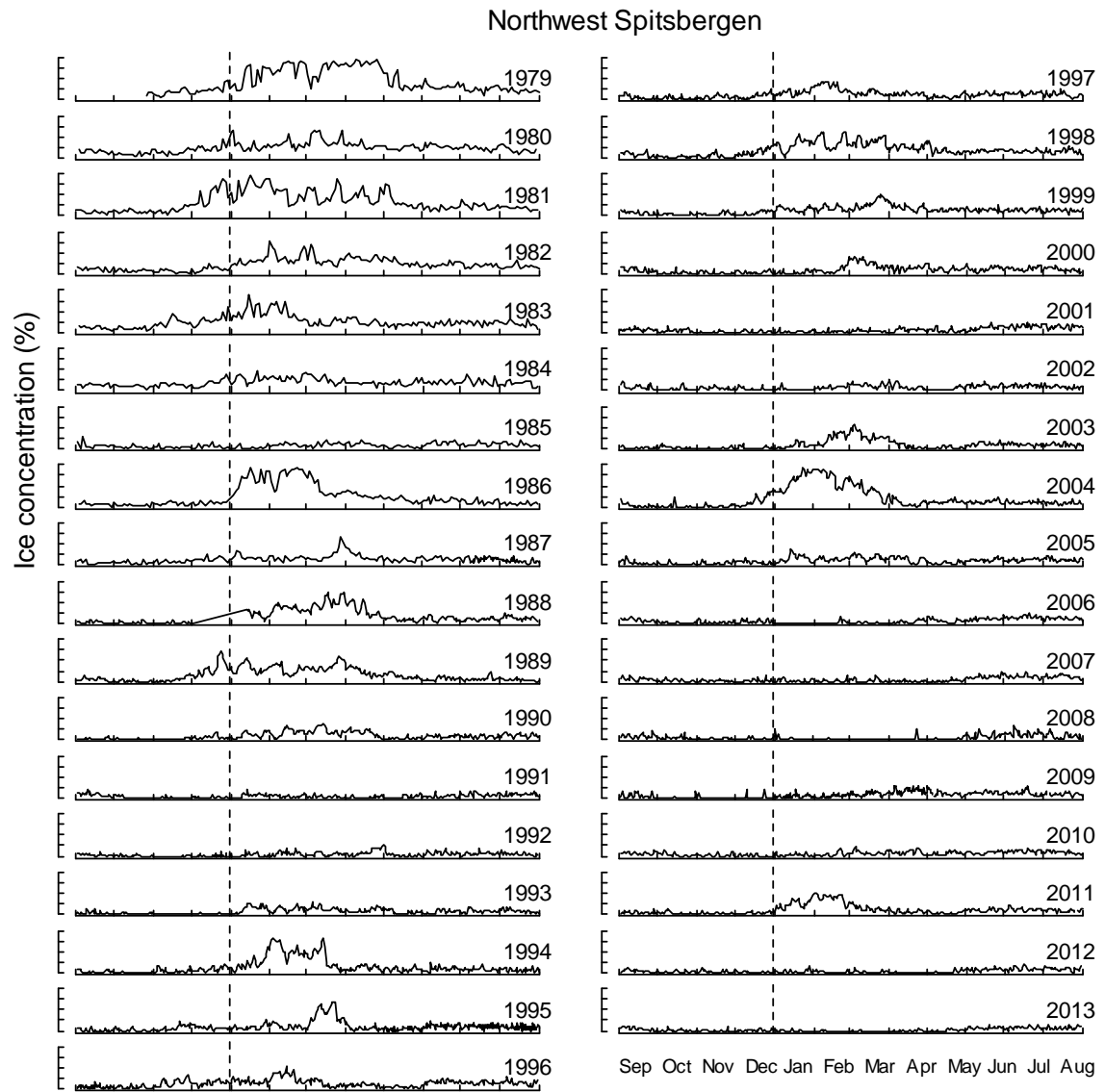
Supplement 2. Sea ice concentrations by date and year for each of the sample areas



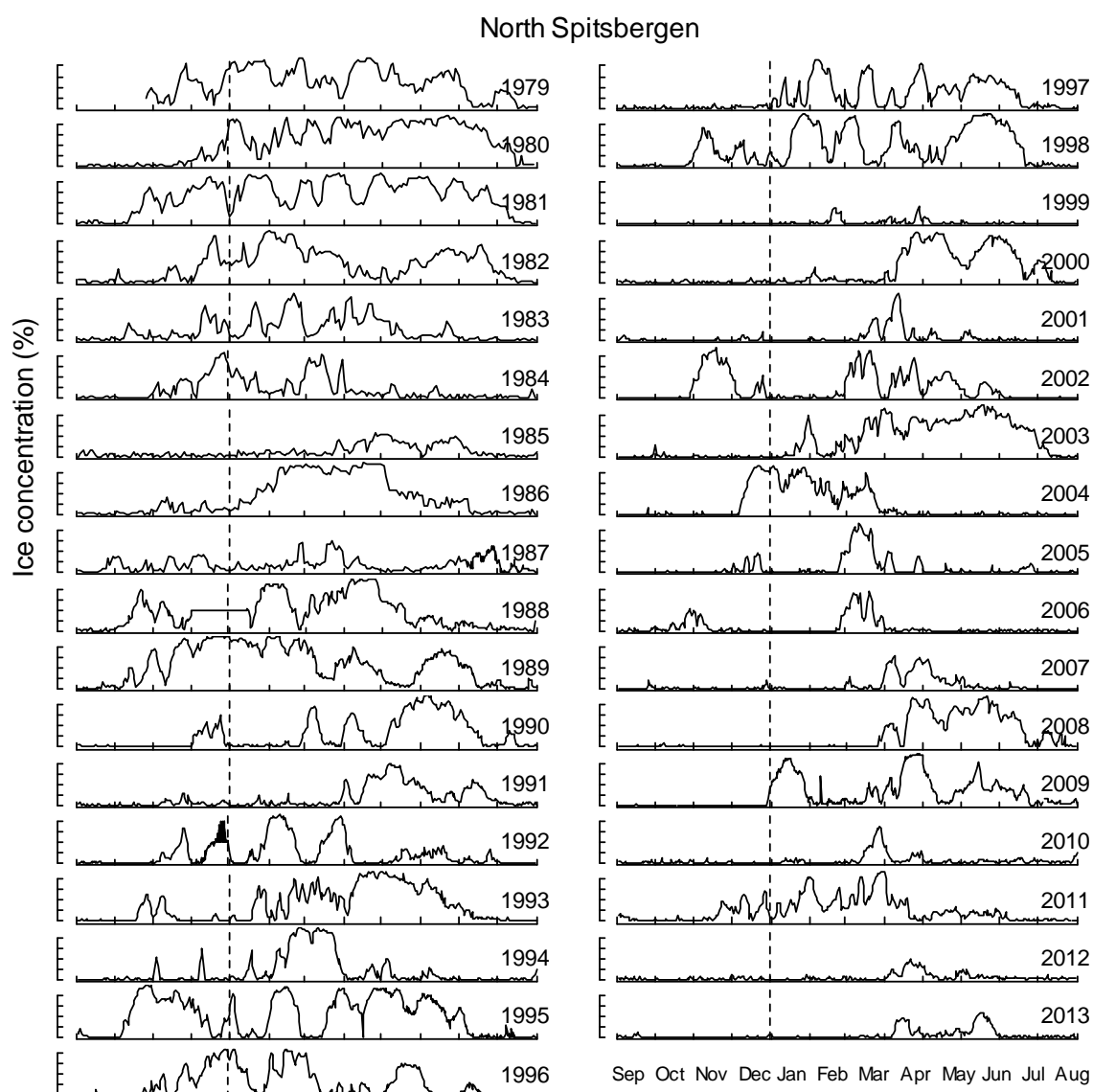
Suppl. 2-Figure S1. Sea ice concentration (%) as a function of date and year at southwest Spitsbergen. The Y-axis ranges 0-100%, and the ticks represents 25, 50 and 75% respectively. Vertical line represents 1 January.



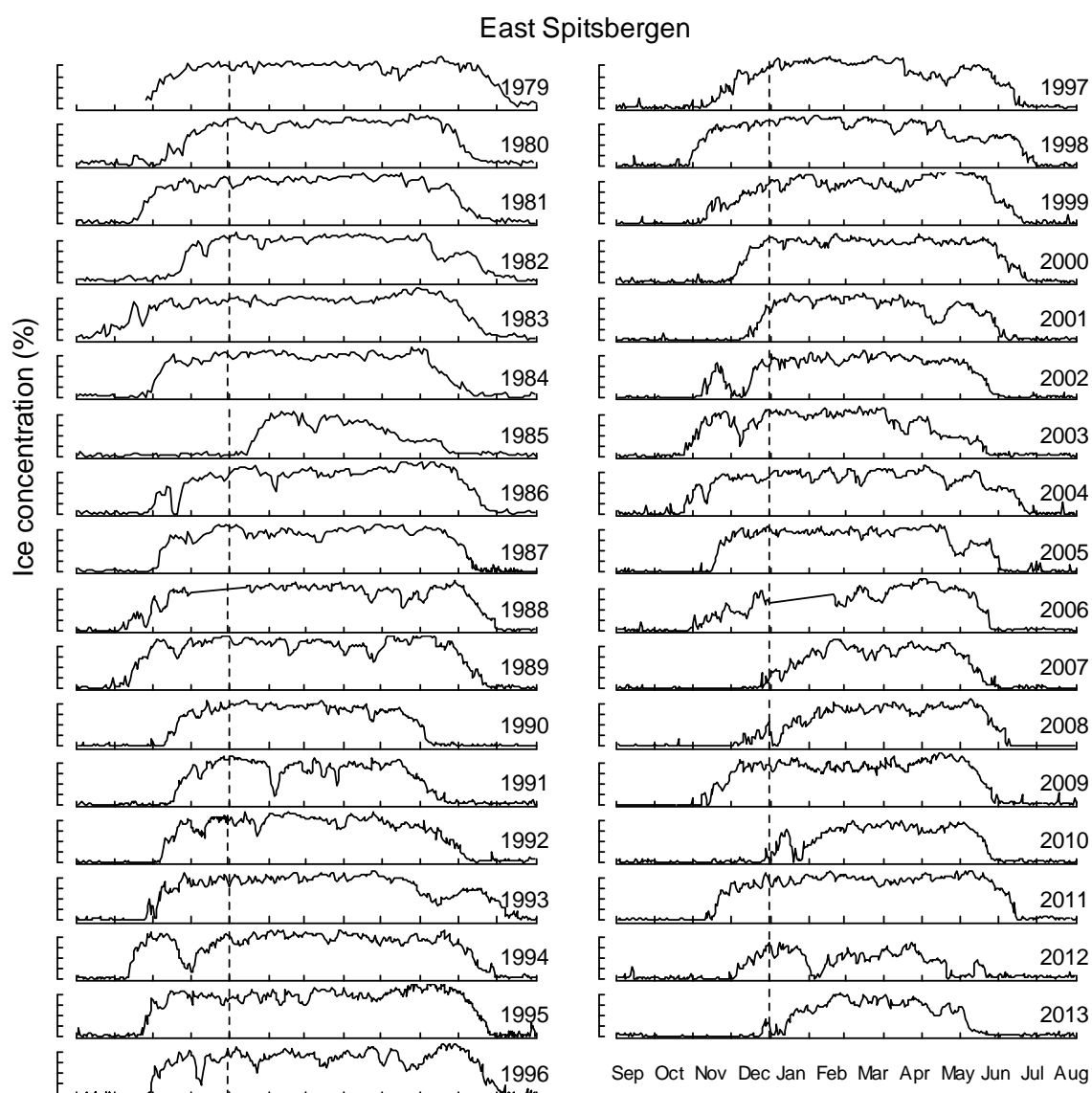
Suppl. 2-Figure S2. Sea ice concentration (%) as a function of date and year at west Spitsbergen. The Y-axis ranges 0-100%, and the ticks represents 25, 50 and 75% respectively. Vertical line represents 1 January.



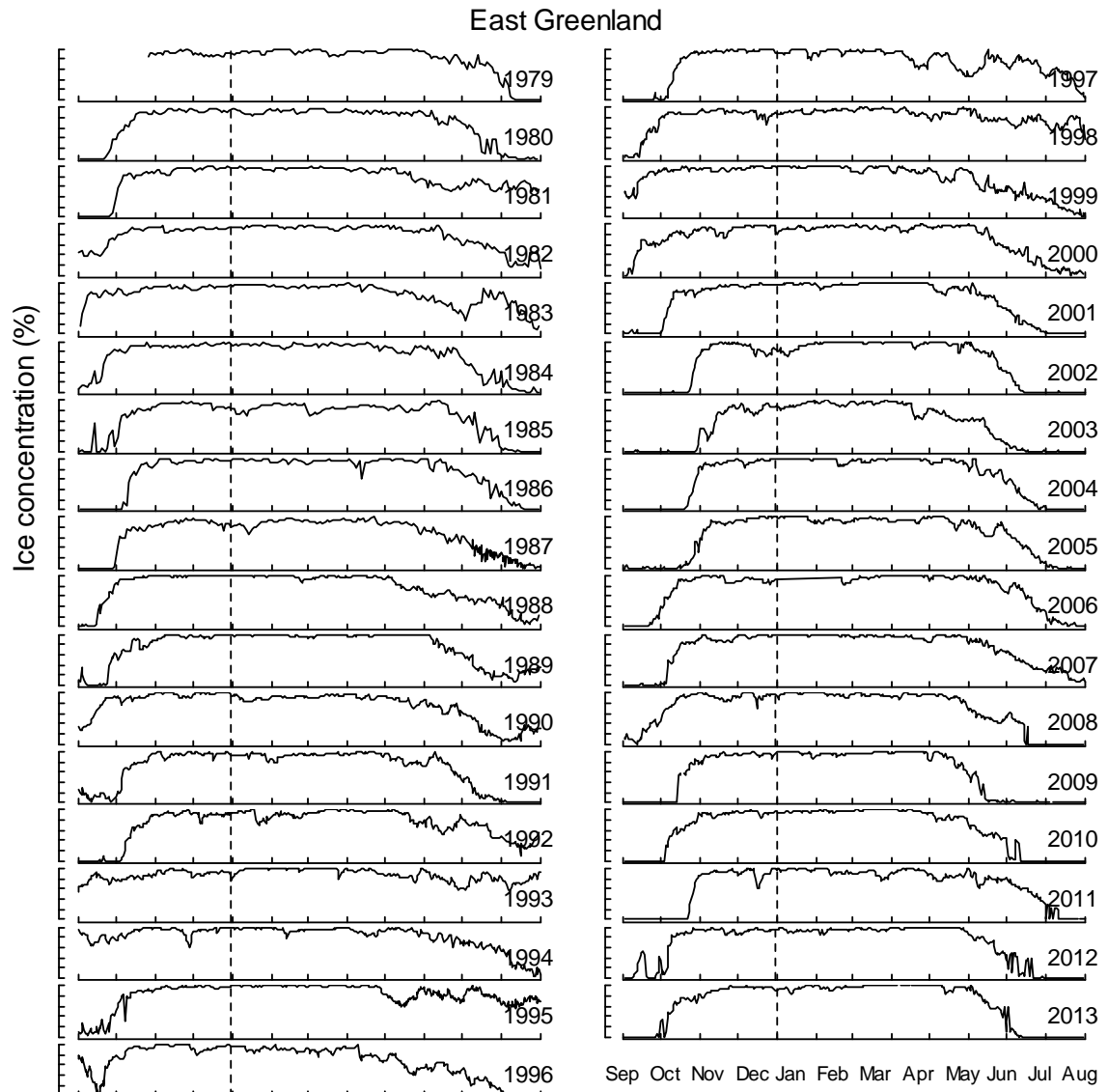
Suppl. 2-Figure S3. Sea ice concentration (%) as a function of date and year at northwest Spitsbergen. The Y-axis ranges 0-100%, and the ticks represents 25, 50 and 75% respectively. Vertical line represents 1 January.



Suppl. 2-Figure S4. Sea ice concentration (%) as a function of date and year at north Spitsbergen. The Y-axis ranges 0-100%, and the ticks represents 25, 50 and 75% respectively. Vertical line represents 1 January.



Suppl. 2-Figure S5. Sea ice concentration (%) as a function of date and year at east Spitsbergen. The Y-axis ranges 0-100%, and the ticks represents 25, 50 and 75% respectively. Vertical line represents 1 January.



Suppl. 2-Figure S6. Sea ice concentration (%) as a function of date and year at east Greenland. The Y-axis ranges 0-100%, and the ticks represents 20, 40, 60 and 80% respectively. Vertical line represents 1 January.

Supplement 3. Statistical trends in ice measures over the years for each sample area.

Suppl. 3-Table S1. Trends in various sea ice indices at southwest Spitsbergen, west Spitsbergen, northwest Spitsbergen, north Spitsbergen, east Spitsbergen and east Greenland, over the period 1979–2013. The indices characterize the length of the sea ice season (Length ICE season 30, days from first to last day with ice concentration $\geq 30\%$), start of ice free season (last day of sea ice $\geq 30\%$), and the monthly mean sea ice concentration (%) for April, May, June and July.

Suppl. 3-Table S1. Annual trends in various sea ice indices at Southwest Spitsbergen, West Spitsbergen, Northwest Spitsbergen, North Spitsbergen, East Spitsbergen and East Greenland, over the period 1979–2013. The indices are the length of the sea ice season (Length ICE season 30, days from first to last day with ice concentration $\geq 30\%$), start of ice free season (last day of sea ice $\geq 30\%$), and the monthly mean sea ice concentration (%) for April, May, June and July.

Southwest Spitsbergen

Statistic	Length ICE season 30 (days)	Start ICE free season 30 (day)	April ICEconc (%)	May ICEconc (%)	June ICEconc (%)	July ICEconc (%)
Slope of trend	−4.238	−1.8235	−0.9	−0.7178	−0.2901	−0.17
SE slope	1.055	0.87	0.22	0.2156	0.165	0.09
Regression R^2	0.31	0.09	0.32	0.23	0.06	0.07
P	0.000319	0.045	0.000245	0.00215	0.0883	0.0727
df	1, 33	1, 33	1, 33	1, 33	1, 33	1, 33
t	−4.018	−2.084	−4.112	−3.329	−1.757	−1.85
Mean	128.6	126.65	28.46	16.587	12.19	7.66
SE mean	12.8	9.26	2.67	2.48	1.72	0.94
Max	273	238	75.8	57.52	40.2	22.9
Min	0	0	1.13	0.1	0.32	0.45

West Spitsbergen

Statistic	Length ICE season 30 (days)	Start ICE free season 30 (day)	April ICEconc (%)	May ICEconc (%)	June ICEconc (%)	July ICEconc (%)
Slope of trend	−3.57	−2.256	−0.843	−0.6465	−0.26473	−0.14
SE slope	0.86	0.74	0.21	0.176	0.078	0.04
Regression R^2	0.32	0.19	0.31	0.27	0.24	−3.4
P	0.000219	0.00466	0.000328	0.00085	0.00177	0.00162
df	1, 33	1, 33	1, 33	1, 33	1, 33	1, 33
t	−4.151	−3.035	−4.009	−3.67	−3.402	−3.4
Mean	82.63	84.34	17.88	9.46	6	4.6
SE mean	10.57	8.36	2.55	2.08	0.9	0.48
Max	211	155	66.79	56.2	20.46	12.3
Min	0	0	0	0	0.36	0.77

Suppl. 3-Table S1.

cont.

Northwest Spitsbergen

Statistic	Length ICE season 30 (days)	Start ICE free season 30 (day)	April ICEconc (%)	May ICEconc (%)	June ICEconc (%)	July ICEconc (%)
Slope of trend	-3.963	-3.9325	-0.8572	-0.497	-0.27716	-0.202
SE slope	0.78	0.73	0.16	0.09	0.06	0.06
Regression R ²	0.42	0.45	0.44	0.45	0.34	0.22
P	0.000015	0.00000573	0.00000943	0.00000701	0.000142	0.0029
df	1, 33	1, 33	1, 33	1, 33	1, 33	1, 33
t	-5.07	-5.4	-5.227	-5.328	-4.3	-3.2
Mean	44.69	59.91	13.15	7.99	10.2	10.4
SE mean	10.37	9.95	2.2	1.27	0.8	0.72
Max	207	188	68.89	30.42	25.2	20.38
Min	0	0	0.1567	0.83	3.19	4.6

North Spitsbergen

Statistic	Length ICE season 30 (days)	Start ICE free season 30 (day)	April ICEconc (%)	May ICEconc (%)	June ICEconc (%)	July ICEconc (%)
Slope of trend	-5.494	-2.04	-0.892	-0.89	-0.8364	-0.65
SE slope	1.095	0.7	0.42	0.43	0.49	0.31
Regression R ²	0.42	0.18	0.09	0.09	0.05	0.09
P	0.0000176	0.00616	0.0419	0.0455	0.0985	0.0452
df	1, 33	1, 33	1, 33	1, 33	1, 33	1, 33
t	-5.016	-2.93	-2.117	-2.079	-1.7	-2.08
Mean	176.49	167.23	37.27	31.74	32.7	17.8
SE mean	14.47	7.78	4.47	4.51	5.1	3.3
Max	305	223	91.41	79.53	89.7	66.2
Min	12	82	1.533	0.46	0.36	0.31

Suppl. 3-Table S1.

cont.

East Spitsbergen

Statistic	Length ICE season 30 (days)	Start ICE free season 30 (day)	April ICEconc (%)	May ICEconc (%)	June ICEconc (%)	July ICEconc (%)
Slope of trend	-1.7146	-0.5812	-0.365	-0.4871	-0.9436	-0.84
SE slope	0.5675	0.2651	0.11	0.2601	0.4	0.28
Regression R ²	0.19	0.1	0.22	-1.873	0.12	0.19
P	0.00484	0.00355	0.00293	0.07	0.023	0.0053
df	1, 33	1, 33	1, 33	1, 33	1, 33	1, 33
t	-3.021	-2.19	-3.21	-1.87	-2.389	-3
Mean	232.14	186.23	76.64	72.44	58.1	20.5
SE mean	6.38	2.82	1.29	2.72	4.26	3.149
Max	295	216	89.92	95.94	92.6	68.7
Min	145	155	53.61	23.58	9.52	1.51

East Greenland

Statistic	Length ICE season 30 (days)	Start ICE free season 30 (day)	April ICEconc (%)	May ICEconc (%)	June ICEconc (%)	July ICEconc (%)
Slope of trend	-1.7527	-1.143	0.131	0.093	-0.4221	-1.101
SE slope	0.5188	0.31	0.068	0.13	0.208	0.34
Regression R ²	0.23	0.26	0.07	0	0.08	0.22
P	0.0019	0.000924	0.06	0.476	0.0502	0.00294
df	1, 33	1, 33	1, 33	1, 33	1, 33	1, 33
t	-3.378	-3.639	1.94	0.72	-2.032	-3.2
Mean	311.9	215.31	94.7	89.32	74.3	44.87
SE mean	5.99	3.7	0.71	1.3	2.19	3.91
Max	366	244	100	99.64	90.8	81.45
Min	239	164	83.2	63.08	26.6	1.92

Supplement 4. Results of statistical modelling

Table S1. Model selection for logistic regression analyses relating the probability of bear encounter to different ICE indices and location. The different ICE indices are described in Supplement 3, Table S1, and the locations are Hornsund, Bellsund, Nordenskiöldkysten, Kongsfjorden and Traill Island. ICE area refers to where the ICE data were extracted (coded as 1 and 2, see Supplement 1, Table S2). Model selection was based on an information theoretic approach, using AICc values. We calculated AICc, Δ AICc and AICc weight for each candidate model according to Burnham and Anderson (2002). Models are ranked by increasing AICc values. See footnote for further descriptions.

rank	model	ICE area	K	AICc	Δ AICc	AICcWt	Cum.Wt
1	Length ICE + loc	2	6	157.2	0	0.46	0.46
2	July ICEconc+ loc	2	6	158.11	0.91	0.29	0.76
3	Length ICE+ loc	1	6	159.34	2.14	0.16	0.92
4	April ICEconc+ loc	1	6	161.06	3.86	0.07	0.99
5	June ICEconc+ loc	2	6	165.51	8.31	0.01	1.00
6	Start ICEfree+ loc	2	6	166.98	9.78	0	1.00
7	Start ICEfree+ loc	1	6	168.29	11.09	0	1.00
8	May ICEconc+ loc	1	6	168.56	11.36	0	1.00
9	June ICEconc+ loc	1	6	169.24	12.04	0	1.00
10	April ICEconc+ loc	2	6	169.53	12.33	0	1.00
11	July ICEconc+ loc	1	6	170.75	13.55	0	1.00
12	May ICEconc+ loc	2	6	172.22	15.02	0	1.00
13	loc	-	5	175.41	18.21	0	1.00

Logistic regression: glm, family=binomial,link=logit.

K is the number of parameters, AICcWt is the AICc weight and Cum.Wt is the cumulative weight.

Burnham, K.P., and Anderson, D.R. (2002). *Model selection and multimodel inference: a practical information-theoretic approach*. Heidelberg: Springer.